# Mechanical Properties of Syndiotactic Propylene−Ethylene Copolymers

**Claudio De Rosa* and Finizia Auriemma**

*Dipartimento di Chimica, Università di Napoli "Federico II", Complesso Monte S. Angelo, Via Cintia, 80126 Napoli, Italy*

*Received June 10, 2005; Revised Manuscript Received October 29, 2005*

ABSTRACT: Syndiotactic propylene−ethylene copolymers have been synthesized with a single-center $C_s$-symmetric syndiospecific metallocene catalyst. The samples show novel thermoplastic elastomeric behavior. Samples with ethylene contents lower than 18−20 mol % are crystalline and show high ductility and remarkable values of the tensile strength. Unoriented compression-molded films of the most crystalline samples, with ethylene contents lower than 6−7 mol %, show poor elastic properties, as in the case of syndiotactic polypropylene, but higher ductility. The elastic properties are improved with increasing ethylene concentration. Stress-relaxed oriented films, instead, present good elastic properties regardless of ethylene concentration. For the most crystalline samples, with ethylene contents lower than 6−7 mol %, the elastic behavior is associated with a reversible polymorphic transition between the *trans*-planar form III and the helical form II that provides an enthalpic contribution to the elasticity. For less crystalline samples, with higher ethylene concentration, the elastic recovery is not associated with any polymorphic transitions and has a pure entropic origin, as in conventional elastomers.

## Introduction

Syndiotactic polypropylene (sPP), despite the high crystallinity, shows unusual elastic properties.[1−4] Unoriented samples of highly crystalline sPP show generally poor elastic properties because of the irreversible plastic deformation occurring during the first stretching.[1−3] Uniaxially oriented fibers show instead good elastic behavior upon successive stretching and relaxation of the samples.[1−4] Elasticity of sPP fibers is generally associated with a reversible polymorphic transition between form II, with chains in 2-fold helical conformation,[5] and form III, characterized by chains in *trans*-planar conformation.[6] The helical form II transforms by stretching into the metastable *trans*-planar form III, which transforms again into the more stable helical form II by releasing the tension,[7] and correspondingly, a total recovery of the initial dimensions of the fiber is observed.[1−4] It has been recently suggested that this stress-induced phase transition is a martensitic phase transformation.[2,4] As in martensitic phase transitions it occurs readily and directly, supporting the idea that elasticity in sPP has a partial enthalpic character, providing an additional contribution to the elastic recovery, besides the entropic contribution as in conventional elastomers.[2,4]

The polymorphism and mechanical properties of sPP samples are strongly influenced by the degree of stereoregularity.[8−10] Recent studies have indicated that low-stereoregular sPP samples with low crystallinity show good elastic behavior at room temperature in a large range of deformation.[8−10]

Large changes in the polymorphism and physical properties of sPP may also be obtained in copolymers of propylene with suitable amounts of other comonomers, as for instance ethylene,[11−17] butene,[11−14,18−21] pentene,[12,13] hexene,[12,13] 4-methyl-1-pentene,[11−13] or octene.[22−25] The effect of the presence of comonomeric units on the polymorphic behavior of sPP has been extensively investigated in as-prepared and melt-crystallized samples of copolymers.[14−20] However, there are only few studies concerning the influence of comonomeric units on the polymorphic behavior of oriented fibers[17,20] and on the mechanical properties of sPP. This issue is of great interest because understanding the role played by constitutional defects on the physical properties of sPP may allow using copolymerization as a tool to finely control physical and mechanical properties of sPP through the tailored introduction of comonomers.

From this point of view copolymers of sPP with ethylene (sPPET) are particularly interesting materials. The copolymer samples are crystalline up to an ethylene content of 18−20 mol %, with melting temperatures decreasing with increasing ethylene content from 150 °C, typical of sPP homopolymer, to nearly 50 °C.[16] Ethylene units are partially included in the crystals of both as-prepared and melt-crystallized samples.[15,16] As-prepared sPPET samples basically crystallize in conformationally disordered modifications of form II of sPP, containing kink bands.[15,16] These modifications are characterized by portions of chains in *trans*-planar conformation in chains having a prevailing 2-fold helical conformation,[26,27] packed as in the isochiral helical form II of sPP.[5,28] These structures are metastable and transform by crystallization from the melt into the most stable disordered helical form I[29] or into the conformationally ordered helical form II, depending on the ethylene concentration.[16]

The effect of the presence of ethylene units on the mechanical properties of sPP has been studied only in oriented fibers.[17] It has been shown that crystalline fibers of sPPET copolymers have good elastic properties regardless of the ethylene concentration.[17]

In this paper the mechanical properties of unoriented samples of sPPET copolymers are investigated in detail and compared with those of oriented films. The elastic behavior shown by oriented films and the mechanical properties of compression-molded films are correlated with the crystallization behavior. This study is aimed at finding relationships between the structure and the mechanical properties of sPPET copolymers and at identifying the mechanisms of elasticity in these materials.

* To whom correspondence should be addressed: Tel ++39 081 674346; Fax ++39 081 674090; e-mail claudio.derosa@unina.it, derosa@chemistry.unina.it.

10.1021/ma051228f CCC: $33.50 
Published on Web 12/03/2005

**Table 1. Composition, Melting Temperature ($T_m$), Intrinsic Viscosity ([$\eta$]), and Average Molecular Mass ($M_v$) of sPPET Copolymer Samples Prepared with the Catalytic System $Ph_2C(Cp)(Flu)ZrCl_2$/MAO[a]**

| sample | feed composition (mol % ethylene) | copolymer composition (mol % ethylene)[b] | $T_m$ (°C)[c] | [$\eta$] (dL/g)[d] | $M_v$[e] |
|---|---|---|---|---|---|
| sPPET(1) | 4.9 | 2.6 | 129.0 | 0.89 | $1.14 \times 10^5$ |
| sPPET(2) | 7.6 | 6.3 | 110.2 | 1.78 | $2.37 \times 10^5$ |
| sPPET(3) | 10.3 | 8.0 | 103.2 | 2.26 | $3.03 \times 10^5$ |
| sPPET(4) | 12.1 | 8.5 | 95.0 | 1.94 | $2.59 \times 10^5$ |
| sPPET(5) | 12.6 | 9.1 | 95.0 | 2.12 | $2.84 \times 10^5$ |
| sPPET(6) | 17.3 | 13.2 | 85.0 | 2.02 | $2.69 \times 10^5$ |
| sPPET(7) | 21.4 | 14.3 | 78.2 | 1.13 | $1.45 \times 10^5$ |
| sPPET(8) | 24.9 | 15.9 | 66.0 | 1.47 | $1.94 \times 10^5$ |
| sPPET(9) | 27.1 | 16.2 | 65.9 | 1.47 | $1.94 \times 10^5$ |
| sPPET(10) | 34.4 | 17.5 | 53.9 | 1.14 | $1.48 \times 10^5$ |
| sPPET(11) | 45.5 | 26.8 | | 1.17 | $1.53 \times 10^5$ |
| sPPET(12) | 71.2 | 47.7 | | 0.89 | $1.14 \times 10^5$ |
| sPPET(13) | 82.5 | 59.1 | | 1.01 | $1.31 \times 10^5$ |

[a] Polymerization temperature = 10 °C; pressure = 1 atm; solvent = toluene (100 mL); molar ratio Al/Zr = 1000; catalyst amount = 2−3 mg; reactor volume = 250 mL; polymerization time = 2 h; flow rate = 5 mL/s; yield = 2−5 g. [b] Determined from $^{13}C$ NMR spectra, recorded with a Varian XL-200 spectrometer operating at 50.3 MHz, of 10% w/v polymer solutions in deuterated tetrachloroethane (also used as internal standard) at 120 °C. [c] Determined from maximum of melting endotherm recorded using a Perkin-Elmer DSC 7 apparatus in $N_2$ atmosphere at 10 °C/min heating rate. [d] Measured in 1,2,3,4-tetrahydronaphthalene solutions at 135 °C. [e] Molecular masses evaluated from values of intrinsic viscosity, using the parameters of Mark−Houwink equation reported for atactic polypropylene $\alpha = 0.96$ and $k = 1.24 \times 10^{-5}$ dL/g.[30]

## Experimental Section

Samples of sPPET copolymers having concentration of ethylene in the range 2−60 mol % have been prepared using the single-center metallocene catalyst (phenyl)$_2$methylen(cyclopentadienyl)-(9-fluorenyl)$ZrCl_2$ ($Ph_2C(Cp)(Flu)ZrCl_2$) activated with methylaluminoxane (MAO), according to the method described in ref 16. All analyzed samples and conditions of polymerization are listed in Table 1.

Unoriented films used for structural analysis and mechanical tests have been obtained by compression-molding of as-polymerized samples. X-ray powder diffraction profiles have been obtained with Ni-filtered Cu K$\alpha$ radiation with an automatic Philips diffractometer. The crystallinity has been evaluated from the X-ray powder diffraction profiles by the ratio of the crystalline diffraction area and the total area of the diffraction profile. The crystalline contribution has been obtained by subtracting from the whole diffraction profile the X-ray diffraction profile of the amorphous phase. The amorphous halo has been obtained from the X-ray diffraction profile of an atactic polypropylene after suitable scaling.

Mechanical tests have been performed at room temperature on compression-molded films and stress-relaxed oriented films of the samples sPPET with a miniature mechanical tester apparatus (Minimat, by Rheometrics Scientific), following the standard test method for tensile properties of thin plastic sheeting ASTM D882-83. Rectangular specimens 10 mm long, 5 mm wide, and 0.3 mm thick of the compression-molded films have been stretched up to the break or up to a given strain $\epsilon$ at constant deformation rate. Two benchmarks have been placed on the test specimens and used to measure elongation.

The values of the tension set and elastic recovery have been measured on compression-molded films after a given strain $\epsilon$ or after breaking according to the standard test method ASTM D412-87. For breaking experiments, specimens of initial length $L_0$ have been stretched up to the break. Ten minutes after breaking the two pieces of the sample have been fit carefully together so that they are in contact over the full area of the break and the final total length $L_r$ of the specimen has been obtained by measuring the distance between the two benchmarks. The tension set at break has been calculated as $t_b = 100(L_r - L_0)/L_0$.

Stress-relaxed oriented films have been prepared by stretching at room temperature specimens of compression-molded films of initial length $L_0$ up to final lengths $L_f = 4L_0$, $6L_0$, and $9L_0$, that is, up to 300, 500, and 800% deformations ($\epsilon = 100(L_f - L_0)/L_0$), keeping the film under tension for 10 min and then removing the tension allowing the relaxation of the sample up to the length $L_r$. The final length of the relaxed specimens $L_r$ is measured after 10 min. For each sample the relaxed length $L_r$ is generally lower than the length $L_f$ achieved during the stretching but higher than the initial length $L_0$ because the elastic recovery of the films after removing the tension is not complete. The tension set and elastic recovery are calculated as $t_s(\epsilon) = 100(L_r - L_0)/L_0$ and $r(\epsilon) = 100-(L_f - L_r)/L_r$, respectively. Oriented films of samples sPPET($n$) of Table 1 stress-relaxed from $\epsilon = 300$, 500, and 800% deformations are identified as samples sPPET($n$)-$\epsilon$. Mechanical cycles of stretching and relaxation have been performed at room temperature on these stress-relaxed films, and the corresponding hystereses have been recorded. In these cycles the stress-relaxed films having the new initial length $L_r$ have been stretched up to the final lengths $L_f = 4L_0$ and $6L_0$ (that is up to the maximum length achieved during the stretching of the starting unoriented film), so that the deformation achieved during the cycles is $\epsilon = 100(L_f - L_r)/L_r$. This precaution was taken in order to avoid further irreversible plastic deformations during the stretching steps. After each cycle, the values of the tension set have been measured. The final length of the relaxed specimens $L_r'$ has been measured 10 min after the end of the relaxation step, and the tension set has been calculated as $t_s(\epsilon) = 100(L_r' - L_r)/L_r$.

## Results and Discussion

**Unoriented Films.** The X-ray powder diffraction profiles of compression-molded films, slowly crystallized from the melt, of sPPET samples are reported in Figure 1. The samples are crystalline up to an ethylene concentration of 18−20 mol %. The degree of crystallinity, evaluated from the X-ray diffraction profiles of Figure 1 and reported in Table 2, decreases with increasing ethylene content.

The X-ray diffraction profiles of sPPET samples with low ethylene contents (lower than 10 mol %, samples sPPET(1)−sPPET(5)) present the 200 and 020 reflections of form I at $2\theta \approx 12°$ and 16°, respectively (Figure 1a−e), indicating that these samples are mainly crystallized in the antichiral helical form I of sPP. Disordered modifications of form I are obtained in these samples, as shown by the absence in the diffraction profiles of Figure 1 of the 211 reflection at $2\theta = 18.8°$, typical of the ordered form I.[29] Structural disorder consists of departures from perfect alternation of right- and left-handed 2-fold helical chains along the $a$ and $b$ axes of the orthorhombic unit cell.[29] In the X-ray diffraction profiles of samples sPPET(2)−sPPET(5) (Figure 1b−e) the peak at $2\theta = 16°$ presents a shoulder at $2\theta = 17°$, corresponding to the 110 reflection of the isochiral helical form II.[5,28] This indicates the presence in these samples of a

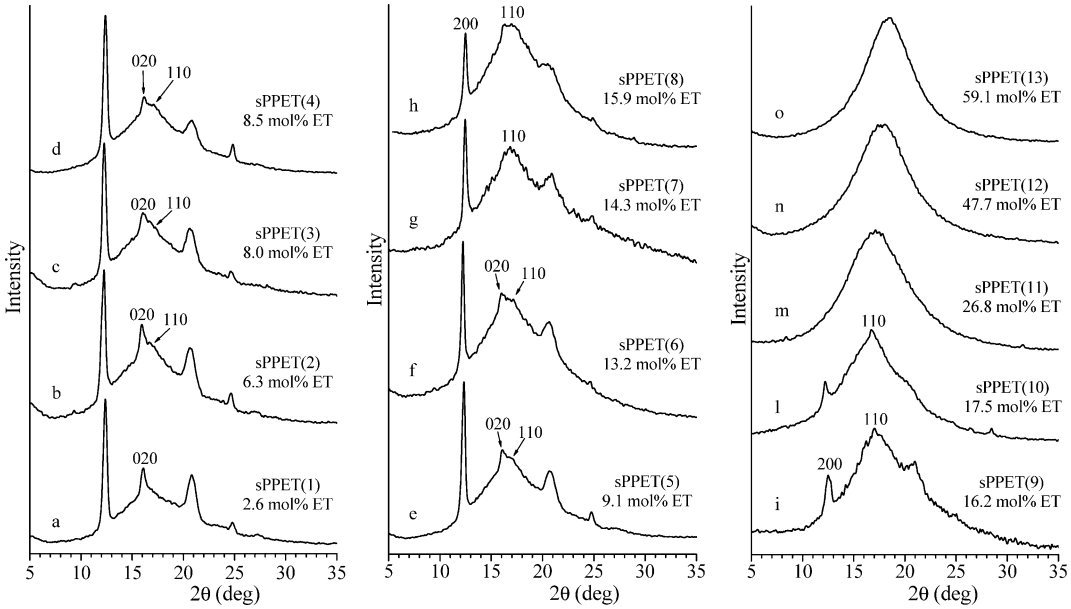


**Figure 1.** X-ray powder diffraction profiles of compression-molded films of sPPET samples of the indicated concentration of ethylene (ET) comonomeric units. The 200 and 020 reflections at $2\theta = 12°$ and 16° of the helical form I and the 110 reflection at $2\theta = 17°$ of the isochiral helical form II are shown.

**Table 2. Young's Modulus ($E$), Stress ($\sigma_y$) and Strain ($\epsilon_y$) at Yield, Stress ($\sigma_b$), Strain ($\epsilon_b$), and Tension Set ($t_b$) at Break, and Crystallinity ($x_c$) of Unoriented Compression-Molded Films of sPPET Samples**

| sample | composition (mol % ethylene) | $E$ (MPa) | $\sigma_y$ (MPa) | $\epsilon_y$ (%) | $\sigma_b$ (MPa) | $\epsilon_b$ (%) | $t_b$ (%) | $x_c$ (%) |
|---|---|---|---|---|---|---|---|---|
| sPPET(1) | 2.6 | 168 ± 22 | 14 ± 1 | 73 ± 13 | 29 ± 5 | (20 ± 1) × 100 | (7 ± 3) × 100 | 48 |
| sPPET(2) | 6.3 | 113 ± 23 | 9 ± 2 | 77 ± 17 | 29 ± 8 | (21 ± 2) × 100 | (9 ± 2) × 100 | 45 |
| sPPET(3) | 8.0 | 67 ± 9 | 8 ± 3 | 78 ± 18 | 26 ± 5 | (23 ± 1) × 100 | (9 ± 1) × 100 | 44 |
| sPPET(4) | 8.5 | 61 ± 8 | 6 ± 1 | 78 ± 14 | 28 ± 4 | (27 ± 3) × 100 | (9 ± 1) × 100 | 42 |
| sPPET(5) | 9.1 | 43 ± 8 | 6 ± 2 | 90 ± 25 | 26 ± 4 | (32 ± 2) × 100 | (10 ± 4) × 100 | 42 |
| sPPET(6) | 13.2 | 32 ± 2 | 5 ± 1 | 99 ± 15 | 26 ± 5 | (40 ± 6) × 100 | (10 ± 1) × 100 | 40 |
| sPPET(7) | 14.3 | 27 ± 3 | 3 ± 1 | 122 ± 27 | 19 ± 5 | (43 ± 5) × 100 | (10 ± 1) × 100 | 38 |
| sPPET(8) | 15.9 | 23 ± 9 | 1.0 ± 0.3 | 158 ± 17 | 15 ± 2 | (50 ± 2) × 100 | (10 ± 2) × 100 | 35 |
| sPPET(9) | 16.2 | 14 ± 7 | 1.0 ± 0.2 | 153 ± 30 | 14 ± 2 | (50 ± 6) × 100 | (8 ± 2) × 100 | 33 |
| sPPET(10) | 17.5 | 7 ± 2 | 1.3 ± 0.4 | 186 ± 36 | 6 ± 3 | (45 ± 4) × 100 | (5 ± 2) × 100 | 25 |
| sPPET(11) | 26.8 | 0.36 ± 0.03 | 0.290 ± 0.009 | 113 ± 12 | 0.33 ± 0.05 | (3.2 ± 0.9) × 100 | | |
| sPPET(12) | 47.7 | 0.12 ± 0.04 | 0.044 ± 0.003 | 63 ± 18 | 0.02 ± 0.01 | (1.2 ± 0.8) × 100 | | |
| sPPET(13) | 59.1 | 0.10 ± 0.02 | 0.040 ± 0.004 | 48 ± 16 | 0.010 ± 0.009 | (1.0 ± 0.8) × 100 | | |

not negligible amount of crystals of the isochiral helical form II of sPP that increases with increasing ethylene content.

The X-ray diffraction profiles of sPPET samples with ethylene content in the range 10−18 mol % (Figure 1f−l) still present reflections centered at $2\theta \approx 12°$, 16°, 17°, and 21°, but the intensity of the 110 reflection at $2\theta = 17°$ of form II tends to increase with respect to that of the 020 reflection at $2\theta = 16°$ of form I with increasing ethylene concentration, indicating an increase of the amount of crystals of form II. In the case of the sample sPPET(6) with ethylene content of 13.2 mol % the maxima at $2\theta = 16°$ and 17° have nearly the same intensity (Figure 1f), whereas sPPET samples with ethylene content in the range 14−18 mol % (samples sPPET(7)−sPPET(10)) the maximum at $2\theta = 16°$ is buried by a broad peak that extends in the $2\theta$ range 15°−19°, with maximum centered at $2\theta = 17°$ (Figure 1g−l). This indicates that these samples are mainly crystallized in modifications close to the isochiral helical form II of sPP. Finally, samples with ethylene content in the range 26−60 mol % (samples sPPET(11)−sPPET(13)) are amorphous (Figures 1m−o).

These data indicate that the presence of even small concentrations of ethylene units, partially included in the crystalline lattice of sPP,[15,16] prevents the crystallization from the melt of the ordered antichiral helical form I of sPP, characterized by order in the alternation of right- and left-handed helical chains along the axes of the unit cell, and induces, at high concentrations, crystallization of the helical form II. The ethylene units are probably better tolerated in the crystalline domains of sPP if the chains are locally packed as in the *C*-centered form II of sPP.[16] In any case highly disordered crystals of form I and form II are obtained from melt-crystallizations.

The stress−strain curves of unoriented compression-molded films of the sPPET samples of Figure 1 are reported in Figure 2. The most important mechanical parameters evaluated from the stress−strain tests of Figure 2 are summarized in Table 2 (Young's modulus, stress and strain at yield, stress and strain at break, tension set at break).

All crystalline sPPET samples (sPPET(1)−sPPET(10)) do not deform homogeneously, and generally, necking is observed (Figure 2A,B). They can be easily stretched up to very high values of deformation, indicating high ductility of the samples. Even when the concentration of ethylene is very small, sPPET copolymers experience values of deformation at break higher than 2000% and much higher than those generally observed for sPP homopolymer samples prepared with the same catalyst and showing similar stereoregularity and crystallinity.[1,3] The high ductility of the crystalline samples is also accompanied by remarkable high values of the tensile strength (Figure 2A,B and Table 2).

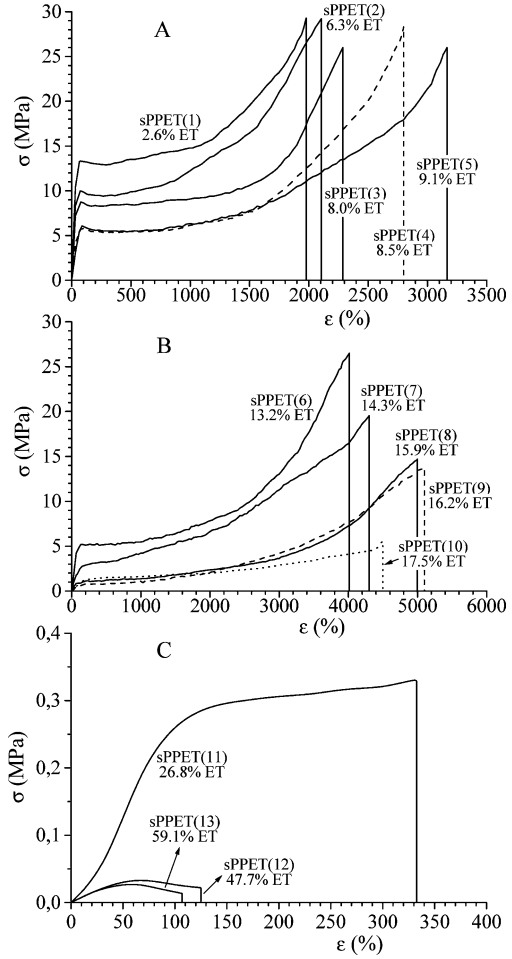


**Figure 2.** Stress−strain curves of semicrystalline (A, B) and amorphous (C) sPPET copolymer samples of the indicated concentration of ethylene (ET) comonomeric units.

The much higher ductility of sPPET copolymers compared to the sPP homopolymer is probably related to the higher flexibility of the polymer chains and the fact that crystals of sPPET samples obtained by melt-crystallizations are much more disordered that those of sPP and hence much more easily deformable. In fact, the presence of ethylene units in part included in the crystals of sPP induces local formation of sequences in *trans*-planar conformation with a consequent increase of chain flexibility.[15,16] It is worth noting that *trans*-planar sequences have also been found in chains of sPP homopolymer samples crystallized in conformationally disordered modifications of form II containing kink bands,[26,27] and the formation of these disordered modifications has been found to be easier in the as-prepared samples of sPPET copolymers than in the case of the sPP homopolymer because it is kinetically favored by the easier local formation of *trans*-planar sequences.[15,16]

Moreover, as shown by the X-ray diffraction profiles of Figure 1, in the melt-crystallized samples of sPPET samples mixtures of disordered crystals of forms I and II are always obtained. The absence of the 211 reflection at $2\theta = 18.8°$ and the broadness of the reflection at $2\theta = 15°-18°$ in the X-ray powder diffraction profiles of Figure 1 at any ethylene concentration indicate that both crystals of form I and form II present structural disorder characterized by stacking faults in the piling of consecutive *bc* layers of 2-fold helical chains along the *a* axis and disorder in the statistical substitution of right- and left-handed helical chains. These disorders induce departures from the fully antichiral packing of the helices in the crystalline domains of form I and departures from the fully isochiral packing of the helices in the crystalline domains of form II. In particular, chains of copolymers containing long propylene constitutional sequences, at low ethylene concentration, basically crystallize in the form I of sPP. The presence of ethylene units, included in these crystals, induces shifts of *bc* layers of chains of $b/4$ along $b$ ($b/4$ shifts disorder, $b = 11.2$ Å for form I),[29] which in turn, prevents the crystallization of the most ordered antichiral modification of form I. Portions of chains containing shorter fully propylene constitutional sequences, with high amounts of ethylene units, tend instead to crystallize mainly in the form II. These crystals include $b/2$ shifts disorder ($b = 5.6$ Å for form II) as well as disorder in the statistical substitution of right- and left-handed helical chains. These disorders produce local arrangements of the chains as in the antichiral form I and induces departures from the fully isochiral packing of form II of sPP.[16] Therefore, at any ethylene concentration and any values of crystallinity, the polymer chains of sPPET copolymers are highly flexible and the crystals are highly disordered and, hence, easily deformable, accounting for the very high ductility of the samples (Figure 2A,B).

Amorphous sPPET samples with ethylene content higher than 26% (samples sPPET(11)−sPPET(13)) deform homogeneously and show poor mechanical properties, with values of stress at any strain and of strain at break drastically reduced with respect to those measured in the case of semicrystalline sPPET samples ($\epsilon_b$ is lower than 350%, Figure 2C and Table 2). The low mechanical strength of the samples sPPET(11)−sPPET(13) is due to the absence of crystallinity (Figure 1m−o). Moreover, these materials experience viscous flow upon application of a small stress, even for a short time, because the molecular masses are not high enough to prevent disentanglement and, then, relative motion of chains (Figure 2C).

It is worth noting that, since the molecular masses of all the analyzed sPPET samples are very similar (Table 1), the great difference in the mechanical behavior of semicrystalline and amorphous samples is only due to the crystallinity. In particular, in the case of the lowest crystalline sample sPPET(10) with 17.5 mol % of ethylene, even though the sample is basically amorphous, the very small level of crystallinity (nearly 25%) achieved by cooling the melt to room temperature is enough to induce very high ductility (deformation at break higher than 4000%) and remarkable values of modulus and tensile strength (7 and 6 MPa, respectively, Table 2) and to prevent viscous flow.

The values of modulus, stress, and strain at yield and at break and crystallinity are reported in Figure 3 as a function of ethylene concentration. It is apparent that Young's modulus, the stress at yield, and the stress at break decrease with increasing ethylene content (Figure 3A,A′,B,B′), according to the decrease of crystallinity (Figure 3D). In particular, the values of tensile strength ($\sigma_b$) is basically constant with the ethylene content up to 13 mol % and then decrease for a further increase of ethylene concentration (Figure 3B,B′). The strain at yield and the stain at break increase up to ethylene content of 18 mol %, i.e., for the semicrystalline samples (Figure 3C), and then rapidly decrease for a further increase of ethylene, i.e., in the case of amorphous samples. These data indicate that sPPET samples become less rigid and more easily deformable with increasing ethylene content.

The experimental evidence that the tensile strength $\sigma_b$ remains constant at high values, while the modulus and the stress at yielding decrease with increasing ethylene content (Figure

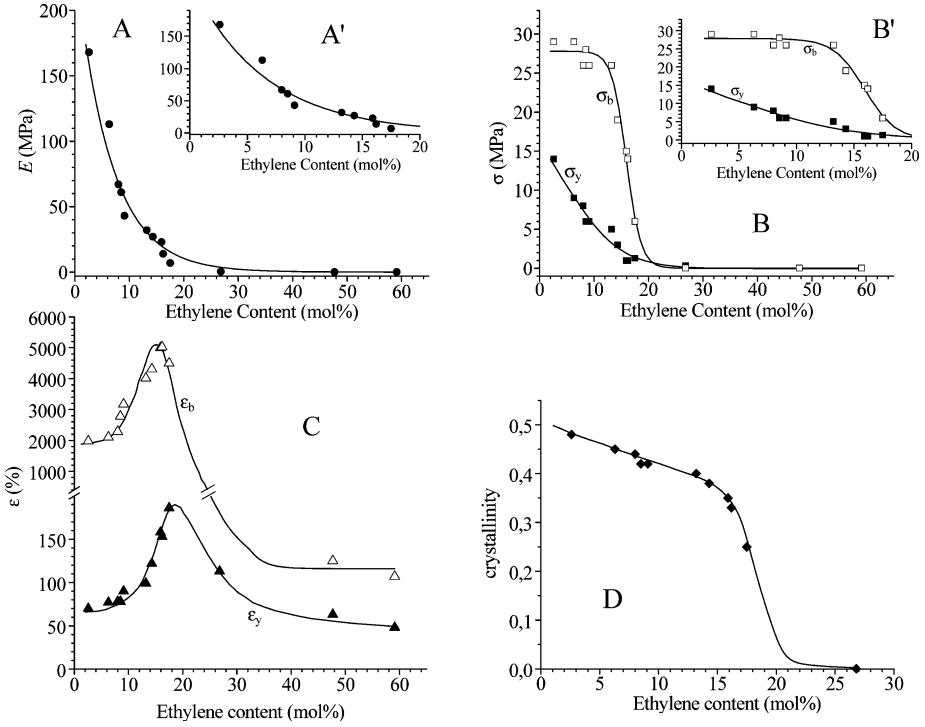


**Figure 3.** Values of Young's modulus (A), stress at yield ($\sigma_y$) and at break ($\sigma_b$) (B), strain at yield ($\epsilon_y$) and at break ($\epsilon_b$) (C), and degree of crystallinity (D) of unioriented compression-molded films of sPPET samples as a function of ethylene content. In insets A′ and B′, the values of Young's modulus and of stress at yield and at break, respectively, of the semicrystalline sPPET samples are reported on an enlarged scale of ethylene concentration.

3A,B), is due to the remarkable strain hardening occurring at high deformations, observed especially for the samples sPPET-(3)−sPPET(6) (Figure 2A,B).

Moreover, the well-defined yielding of the most crystalline samples sPPET(1)−sPPET(6) is reduced with increasing ethylene content and decreasing crystallinity (Figure 3D), so that the stress−strain curves of the less crystalline samples sPPET-(7)−sPPET(10) present the typical shape of thermoplastic elastomers (Figure 2B). The values of tension set at break $t_b$, which give the residual deformation after breaking, are, indeed, much lower than the values of deformation at break (Table 2), indicating a partial elastic recovery after breaking. However, the absolute values of tension set at break are rather high in all cases (Table 2), indicating poor elastic properties after breaking.

The values of tension set of semicrystalline sPPET samples after deformation $\epsilon$, evaluated by stretching the unoriented compression-molded films up to $\epsilon = 300$, 500, and 800% and then removing the tension, are reported in Figure 4 as a function of ethylene content and in Table 3 along with the elastic recovery $r(\epsilon)$. The measured values of tension set are in the range 30−300%, indicating that these materials, in the unoriented state, are only partially elastic. However, for a given deformation, the values of tension set decrease with increasing ethylene content, so that an improvement of elastic behavior is observed for samples with high ethylene concentrations, in the range 16−18 mol % (Figure 4). Moreover, for a given sample, the tension set increases with increasing the maximum deformation achieved during stretching.

These data clearly indicate that unoriented samples of sPPET copolymers show rather good elastic properties for ethylene concentration in the range 16−18 mol %. For lower ethylene content the degree of crystallinity is too high (Figure 3D), and the samples experience irreversible plastic deformation (Figure 2A). For ethylene content higher than 18 mol %, sPPET copolymers are amorphous with no measurable values of tension

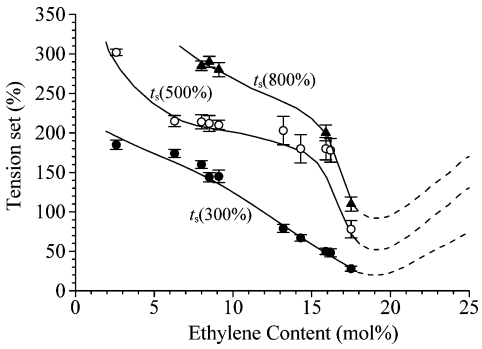


**Figure 4.** Values of tension set $t_s(\epsilon)$ of unoriented compression-molded films of semicrystalline sPPET samples after deformation $\epsilon = 300$ (●), 500 (○), and 800% (▲) as a function of ethylene content. For amorphous sPPET samples with ethylene contents higher than 18−20 mol % the tension set is not measurable (dashed lines) because of occurrence of viscous flow during stretching, and no elastic behavior is observed.

set due to occurrence of viscous flow upon stretching (Figure 2C). For ethylene concentration in the range 16−18 mol %, the small level of crystallinity and the presence of small crystals in disordered helical forms (Figure 1i−l) produce an efficient elastomeric network, and only a small irreversible plastic deformation occurs during stretching. We recall that highly stereoregular sPP homopolymer samples prepared with the same catalyst show only poor elastic properties in the unstretched state;[1−3] therefore, the presence of ethylene units for concentrations in the range 16−18 mol % strongly enhances the elasticity of sPP.

**Oriented Samples.** Stress-relaxed oriented films of the samples sPPET have been obtained by stretching compression-molded films up to a given deformation $\epsilon$ and, then, removing the tension. X-ray diffraction analysis has shown that during stretching of compression-molded films the helical forms present in the unoriented samples (Figure 1) transform into the *trans*-planar forms (form III or mesomorphic form) of sPP, and a

**Table 3. Values of Tension Set ($t_s(\epsilon)$) and Elastic Recovery ($r(\epsilon)$) of Unoriented Compression-Molded Films of sPPET Samples Stretched up to Deformations $\epsilon$ of 300, 500, and 800%**

| sample | composition (mol % ethylene) | $t_s(300)$ (%) | $r(300)$ (%) | $t_s(500)$ (%) | $r(500)$ (%) | $t_s(800)$ (%) | $r(800)$ (%) |
|---|---|---|---|---|---|---|---|
| sPPET(1) | 2.6 | 185 ± 6 | 40 ± 6 | 302 ± 4 | 49 ± 4 | n.d.[a] | n.d.[a] |
| sPPET(2) | 6.3 | 174 ± 5 | 46 ± 5 | 215 ± 7 | 90 ± 7 | n.d.[a] | n.d.[a] |
| sPPET(3) | 8.0 | 160 ± 5 | 54 ± 5 | 214 ± 9 | 91 ± 9 | 285 ± 6 | 134 ± 6 |
| sPPET(4) | 8.5 | 144 ± 6 | 64 ± 6 | 212 ± 10 | 92 ± 10 | 290 ± 7 | 131 ± 7 |
| sPPET(5) | 9.1 | 145 ± 8 | 63 ± 6 | 210 ± 6 | 93 ± 6 | 280 ± 9 | 137 ± 9 |
| sPPET(6) | 13.2 | 79 ± 5 | 123 ± 5 | 203 ± 18 | 98 ± 18 | n.d.[a] | n.d.[a] |
| sPPET(7) | 14.3 | 67 ± 4 | 139 ± 4 | 180 ± 18 | 114 ± 18 | n.d.[a] | n.d.[a] |
| sPPET(8) | 15.9 | 50 ± 4 | 167 ± 4 | 180 ± 14 | 101 ± 14 | 200 ± 10 | 200 ± 10 |
| sPPET(9) | 16.2 | 48 ± 5 | 179 ± 5 | 178 ± 15 | 100 ± 15 | n.d.[a] | n.d.[a] |
| sPPET(10) | 17.5 | 28 ± 3 | 213 ± 3 | 78 ± 11 | 237 ± 11 | 110 ± 9 | 328 ± 9 |

[a] n.d. = not determined.

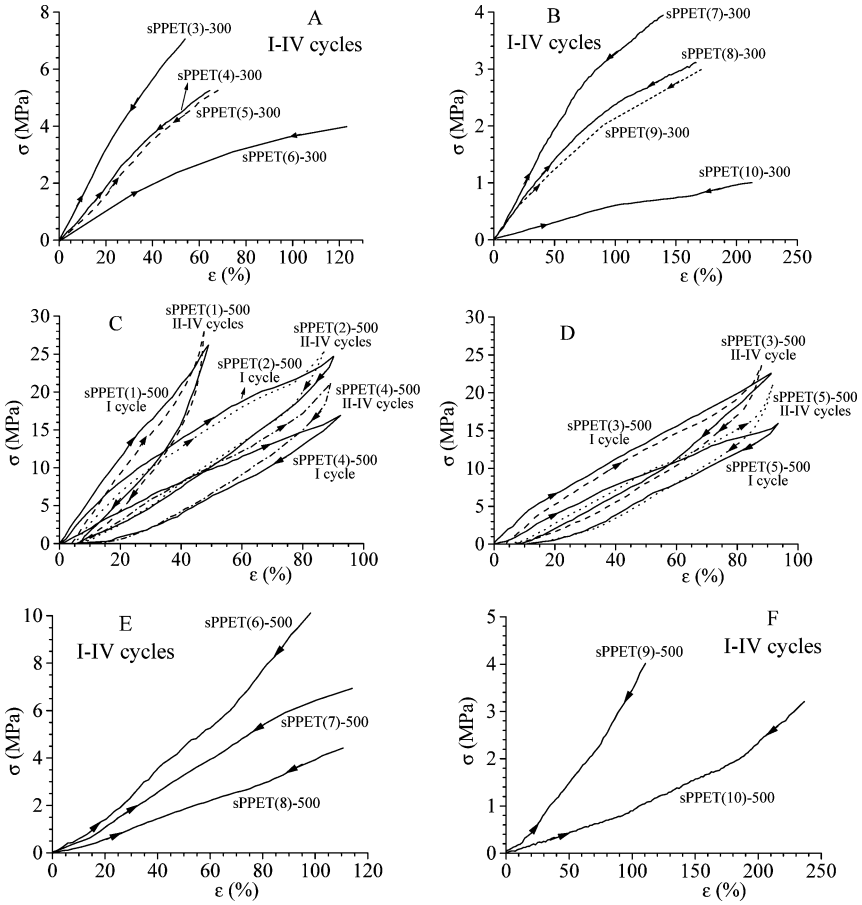


**Figure 5.** Stress−strain hysteresis cycles composed of the stretching and relaxation steps (at controlled rate) according to the direction of the arrows of stress-relaxed oriented films sPPET(*n*)-300 (A, B) and sPPET(*n*)-500 (C−F) of the sPPET samples. In (A) and (B) for all the sPPET(*n*)-300 samples the curves corresponding to the stretching and relaxation steps are coincident (null hysteresis) regardless of the ethylene concentration; therefore, the reported curves are averaged over four consecutive cycles (practically coincident). The hysteresis curves of oriented films sPPET(*n*)-500 of the samples having ethylene contents lower than 10 mol % ($n$ = 1−5) are shown in (C) and (D), whereas those of samples having ethylene contents in the range 10−18 mol % ($n$ = 6−10) are shown in (E) and (F). In (C) and (D) for each sample the first cycles (continuous lines) and curves averaged over the successive II−IV cycles (dashed and dotted lines) are reported. For the samples in (E) and (F) the curves corresponding to the stretching and relaxation steps are coincident (null hysteresis); therefore, the reported curves are averaged over four consecutive cycles (practically coincident). The stress-relaxed films have been prepared by stretching compression-molded films of the samples sPPET(*n*) at 300 and 500% deformation (final length $L_f = 4L_0$ and $6L_0$, with $L_0$ the initial length of the compression-molded film) and then removing the tension.

high fiber orientation of crystals is obtained.[17] After releasing the tension the stress-relaxed films still show high degrees of orientation of crystals.[17] Preliminary analysis of mechanical properties has shown that all stress-relaxed oriented films present elastic behavior.[17] In fact, once the samples have experienced irreversible plastic deformation during stretching of unoriented specimens (Figure 2) and a high degree of orientation has been achieved, the obtained oriented films show elastic properties. However, elasticity and, in particular, the range of deformation where oriented films experience perfect elastic behavior depend on the maximum deformation $\epsilon$ achieved during the stretching of the unoriented samples. For this reason we have studied the elastic properties of different oriented films prepared by stretching compression-molded films of initial length $L_0$ up to deformations $\epsilon$ = 300, 500, and 800% (final lengths $L_f = 4L_0$, $6L_0$, and $9L_0$, respectively) and then removing the tension allowing the relaxation of the films up to the relaxed length $L_r$ (samples sPPET(*n*)-$\epsilon$).

The stress−strain hysteresis cycles, composed of the curves recorded during the stretching and the successive relaxation, of stress-relaxed oriented films sPPET(*n*)-300 and sPPET(*n*)-500 are reported in Figure 5. In these cycles, stress-relaxed oriented

**Table 4. Values of Tension Set ($t_s$) Measured after Stretching Stress-Relaxed Oriented Films sPPET(*n*)-300, sPPET(*n*)-500, and sPPET(*n*)-800 up to the Indicated Maximum Strain ($\epsilon_{max}$) during the First Mechanical Hysteresis Cycle of the Kind of Figure 5 and of Dissipated Energy ($\Gamma_{diss}$) Measured after the First Cycle and after the Successive II−IV Cycles[a]**

| fiber | composition (mol % ethylene) | $t_s(\epsilon_{max})$ | $\epsilon_{max}$ (%)[b] | $\Gamma_{diss}$ (%) (I cycle) | $\Gamma_{diss}$ (%) (II−IV cycle) |
|---|---|---|---|---|---|
| sPPET(1)-300 | 2.6 | 0 | 40 | 0 | 0 |
| sPPET(1)-500 | 2.6 | 4 | 49 | 34 ± 1 | 33 ± 1 |
| sPPET(2)-300 | 6.3 | 0 | 46 | 0 | 0 |
| sPPET(2)-500 | 6.3 | 4 | 90 | 32 ± 2 | 27 ± 3 |
| sPPET(3)-300 | 8.0 | 0 | 54 | 0 | 0 |
| sPPET(3)-500 | 8.0 | 4 | 91 | 30 ± 3 | 29 ± 2 |
| sPPET(3)-800 | 8.0 | 14 | 134 | n.d.[c] | n.d.[c] |
| sPPET(4)-300 | 8.5 | 0 | 64 | 0 | 0 |
| sPPET(4)-500 | 8.5 | 6 | 92 | 30 ± 5 | 29 ± 4 |
| sPPET(4)-800 | 8.5 | 12 | 131 | n.d.[c] | n.d.[c] |
| sPPET(5)-300 | 9.1 | 0 | 63 | 0 | 0 |
| sPPET(5)-500 | 9.1 | 5 | 93 | 30 ± 3 | 29 ± 3 |
| sPPET(5)-800 | 9.1 | 14 | 137 | n.d.[c] | n.d.[c] |
| sPPET(6)-300 | 13.2 | 0 | 123 | 0 | 0 |
| sPPET(6)-500 | 13.2 | 0 | 98 | 0 | 0 |
| sPPET(7)-300 | 14.3 | 0 | 139 | 0 | 0 |
| sPPET(7)-500 | 14.3 | 0 | 114 | 0 | 0 |
| sPPET(8)-300 | 15.9 | 0 | 167 | 0 | 0 |
| sPPET(8)-500 | 15.9 | 0 | 101 | 0 | 0 |
| sPPET(8)-800 | 15.9 | 0 | 200 | 0 | 0 |
| sPPET(9)-300 | 16.2 | 0 | 179 | 0 | 0 |
| sPPET(9)-500 | 16.2 | 0 | 100 | 0 | 0 |
| sPPET(10)-300 | 17.5 | 0 | 213 | 0 | 0 |
| sPPET(10)-500 | 17.5 | 0 | 237 | 0 | 0 |
| sPPET(10)-800 | 17.5 | 0 | 328 | 0 | 0 |

[a] The stress-relaxed oriented films sPPET(*n*)-*x* have been prepared by stretching compression-molded films at $x = 300$, 500, and 800% deformation, respectively (final lengths $L_f = 4L_0$, $6L_0$, and $9L_0$, respectively, with $L_0$ the initial length) and then removing the tension. [b] Values numerically equal to the elastic recovery of unoriented films stretched at 300, 500, and 800% deformations and then relaxed, reported in Table 3. [c] n.d. = not determined.

films having the new initial length $L_r$ are stretched up to the final length $L_f$ ($L_f = 4L_0$ for the samples sPPET(*n*)-300 in Figure 5A,B and $L_f = 6L_0$ for the samples sPPET(*n*)-500 in Figure 5C−F), that is, up to the maximum length achieved during the stretching of the starting unoriented film, so that the maximum deformation achieved during the first cycle ($\epsilon = 100(L_f - L_r)/L_r$) for each sample is numerically equal to the elastic recovery *r*(300) and *r*(500) reported in Table 3. Since the initial length of the stress-relaxed films $L_r$ is higher than the initial length $L_0$ of the unoriented starting film, due to the fact that the elastic recovery after the first stretching of the unoriented film is not complete (see Figure 4), the maximum values of deformation in the hysteresis cycles of Figure 5 are lower than 300 and 500%, being in the range 100−250%. However, each film sPPET(*n*)-500 of Figure 5C−F has been actually stretched up to the final length $L_f = 6L_0$, that is, 500% deformation with respect to the length of the starting unoriented film. These values of the maximum deformation in the stretched steps of the cycles of Figure 5 (final lengths always $L_f = 4L_0$ and $6L_0$) were chosen in order to avoid further irreversible plastic deformations during the stretching steps. For each oriented film at least four consecutive hysteresis cycles have been recorded; each cycle has been performed 10 min after the end of the previous cycle.

It is apparent from Figure 5A,B that the stress−strain curves recorded while cyclically stretching and releasing the tension of stress-relaxed films sPPET(*n*)-300 are nearly coincident, indicating a negligible hysteresis. Moreover, for all samples, the curves recorded during the first cycle coincide with those recorded during the successive cycles, and a total recovery of sample dimensions is observed, the values of tension set being equal to zero already after the first cycle.

The stress-relaxed oriented films sPPET(*n*)-500, instead, present a different behavior depending on the ethylene content. The hysteresis cycles of stress-relaxed films sPPET(*n*)-500 of samples with ethylene content lower than 10 mol %, (samples sPPET(1)−sPPET(5)) are shown in Figure 5C,D. For these samples the values of tension set and of the dissipated energy are nonnull during the first cycle. The stress−strain curves recorded during successive consecutive hysteresis cycles coincide (Figure 5C,D), the values of tension set being nearly equal to zero. The values of tension set after the first cycle and the values of dissipated energy during each cycle are reported in Table 4. The values of dissipated energy are in all cases lower than 35%.

The stress−strain hysteresis curves of stress-relaxed films sPPET(*n*)-500 of sPPET samples with ethylene content in the range 10−18 mol % (samples sPPET(6)−sPPET(10)) are shown in Figure 5E,F. For these samples the stress−strain curves recorded in four successive cycles are nearly coincident, the values of tension set and hysteresis being equal to zero (see Table 4) already after the first cycle (Figure 5E,F). It is also apparent from Figure 5 and Table 4 that the deformation range where sPPET oriented films show elastic behavior increase with increasing the maximum deformation achieved during the stretching of the unoriented specimens and increasing concentration of ethylene.

As demonstrated in our previous structural analysis,[17] the plastic deformation and the elastic recovery of sPPET samples are associated with polymorphic transitions occurring during stretching and relaxation. In unoriented copolymer samples with low ethylene contents the irreversible plastic deformation occurring by stretching is associated with a stress-induced phase transition from the helical form I into the *trans*-planar form III. In the mechanical cycles of Figure 5C, the *trans*-planar form III obtained by stretching transforms into the helical form II during relaxation and elastic recovery.[17] This phase transition is reversible, and the oriented samples show elastic behavior (Figure 5C). It has been suggested that this polymorphic transition provides an enthalpic contribution to the elasticity.[17]

Lower crystalline sPPET samples with higher ethylene concentrations (higher than 10 mol %) show similar elastic properties that are not associated with any polymorphic transitions.[17] These samples show high ductility and elastic behavior even in the unstretched state (Figures 2 and 4). The elastic properties are then improved in oriented fibers (Figure 5E,F). During stretching the helical forms present in the unoriented film transform into the *trans*-planar mesomorphic form, which is stable and does not transform into helical forms during recovery upon releasing the tension.[17] Therefore, elasticity in sPPET samples with ethylene content in the range 10−18 mol % (Figure 5E,F) has a purely entropic origin.[17] The mesomorphic crystalline aggregates present in a mainly amorphous matrix act as physical knots of the elastomeric network, preventing the viscous flow of the chains, as in the case of conventional thermoplastic elastomers. The presence of the crystals warrants for values of stress at any strain and of elastic modulus 1 order of magnitude higher than those of conventional elastomers. Moreover, since the crystals are in the mesomorphic form, they are easily deformable, so that novel elastomeric materials with remarkable value of strength and outstanding ductility are produced.

## Conclusions

Novel thermoplastic elastomeric materials based on syndiotactic propylene−ethylene copolymers, with ethylene concentration variable in the range 2−60 mol %, have been produced.

Samples with ethylene content lower than 18−20 mol % are crystalline and show interesting mechanical properties, whereas samples with ethylene content higher than 20% are amorphous and experience rapid viscous flow even for low deformation and/or by application of stress for long time.

Unoriented films of the crystalline sPPET samples with ethylene content lower than 18 mol % present high ductility and remarkable values of the tensile strength. The elastic modulus and the stress at any strain decrease with increasing ethylene content, consistent with the decrease of crystallinity, whereas the tensile strength remain nearly constant up to ethylene contents of 14−15% because of the strong strain hardening which occurs at high deformations. The most crystalline samples, with low ethylene content, show poor elastic properties because of the irreversible plastic deformation occurring during stretching of unoriented films. The elastic properties are greatly improved for the lowest crystalline samples with ethylene contents in the range 16−18 mol %.

Oriented films of all sPPET samples show good elastic properties regardless of the ethylene concentration. The presence of crystalline domains ensures values of modulus and tensile strength higher than those of conventional elastomers. The elastic behavior of most crystalline sPPET copolymer samples with low ethylene contents (lower than 6−7 mol %) is associated with a reversible polymorphic transition between the *trans*-planar form III and the helical form II occurring during stretching and relaxation cycles. In these samples elasticity has a mainly enthalpic character due to the metastability of the *trans*-planar form III that transforms into the more stable helical form II upon releasing the tension. Lower crystalline sPPET samples with higher ethylene concentrations (higher than 10 mol %) show similar elastic properties, which are not associated with any polymorphic transitions. In these samples the *trans*-planar forms are stable and do not transform into helical forms during elastic recovery, and elasticity has a pure entropic origin as in conventional elastomers.

Syndiotactic propylene−ethylene copolymers prepared with $C_s$-symmetric metallocene catalysts represent new materials with improved and unprecedented mechanical properties of thermoplastic elastomers, whose physical properties and values of mechanical parameters can be finely tuned through the simple introduction of the proper amount of ethylene comonomer units.

**Acknowledgment.** Financial support from the "Ministero dell'Istruzione, dell'Università e della Ricerca" of Italy (PRIN 2004 projects), is gratefully acknowledged. We thank Dr. Giovanni Talarico for the synthesis of the samples.

## References and Notes

(1) Auriemma, F.; Ruiz de Ballesteros, O.; De Rosa, C. *Macromolecules* **2001**, *34*, 4485.
(2) De Rosa, C.; Gargiulo, M. C.; Auriemma, F.; Ruiz de Ballesteros, O.; Razavi, A. *Macromolecules* **2002**, *35*, 9083.
(3) Auriemma, F.; De Rosa, C. *Macromolecules* **2003**, *36*, 9396.
(4) Auriemma, F.; De Rosa, C. *J. Am. Chem. Soc.* **2003**, *125*, 13143.
(5) Corradini, P.; Natta, G.; Ganis, P.; Temussi, P. A. *J. Polym. Sci., Part C* **1967**, *16*, 2477.
(6) Chatani, Y.; Maruyama, H.; Noguchi, K.; Asanuma, T.; Shiomura, T. *J. Polym. Sci., Part C* **1990**, *28*, 393.
(7) De Rosa, C.; Auriemma, F.; Vinti, V. *Macromolecules* **1998**, *31*, 7430.
(8) De Rosa, C.; Auriemma, F.; Ruiz de Ballesteros, O.; Resconi, L.; Fait, A.; Ciaccia, E.; Camurati, E. *J. Am. Chem. Soc.* **2003**, *125*, 10913.
(9) De Rosa, C.; Auriemma, F.; Ruiz de Ballesteros, O. *Macromolecules* **2003**, *36*, 7607.
(10) De Rosa, C.; Auriemma, F.; Ruiz de Ballesteros, O. *Macromolecules* **2004**, *37*, 1422.
(11) Galimberti, M.; Albizzati, E.; Mazzocchi, R. U.S. Patent 5196496, 1993.
(12) Kakugo, M. *Macromol. Symp.* **1995**, *89*, 545.
(13) Naga, N.; Mizunuma, K.; Sadatoshi, H.; Kakugo, M. *Macromolecules* **1997**, *30*, 2197; *Polymer* **2000**, *41*, 203.
(14) De Rosa, C.; Auriemma, F.; Vinti, V.; Grassi, A.; Galimberti, M. *Polymer* **1998**, *39*, 6219.
(15) De Rosa, C.; Auriemma, F.; Talarico, G.; Busico, V.; Caporaso, L.; Capitani, D. *Macromolecules* **2002**, *35*, 1314.
(16) De Rosa, C.; Auriemma, F.; Fanelli, E.; Talarico, G.; Capitani, D. *Macromolecules* **2003**, *36*, 1850.
(17) De Rosa, C.; Auriemma, F. *Adv. Mater.* **2005**, *17*, 1503.
(18) De Rosa, C.; Talarico, G.; Caporaso, L.; Auriemma, F.; Fusco, O.; Galimberti, M. *Macromolecules* **1998**, *31*, 9109.
(19) De Rosa, C.; Auriemma, F.; Caporaso, L.; Talarico, G.; Capitani, D. *Polymer* **2000**, *41*, 2141.
(20) De Rosa, C.; Auriemma, F.; Orlando, I.; Talarico, G.; Caporaso, L. *Macromolecules* **2001**, *34*, 1663.
(21) Zhang, B.; Yang, D.; De Rosa, C.; Yan, S. *Macromolecules* **2002**, *35*, 4646.
(22) Jungling, S.; Mulhaupt, R.; Fisher, D.; Langhauser, F. *Angew. Makromol. Chem.* **1995**, *229*, 93.
(23) Thomann, R.; Kressler, J.; Mulhaupt, R. *Macromol. Chem. Phys.* **1997**, *198*, 1271.
(24) Thomann, R.; Kressler, J.; Mulhaupt, R. *Polymer* **1998**, *39*, 1907.
(25) Hauser, G.; Schmidtke, J.; Strobl, G. *Macromolecules* **1998**, *31*, 6250.
(26) Auriemma, F.; Born, R.; Spiess, H. W.; De Rosa, C.; Corradini, P. *Macromolecules* **1995**, *28*, 6902.
(27) Auriemma, F.; Lewis, R. H.; Spiess, H. W.; De Rosa, C. *Macromol. Chem.* **1995**, *196*, 4011.
(28) De Rosa, C.; Corradini, P. *Macromolecules* **1993**, *26*, 5711.
(29) De Rosa, C.; Auriemma, F.; Vinti, V. *Macromolecules* **1997**, *30*, 4137.
(30) Brandrup, J.; Immergut, E. H.; Grulke, E. A. *Polymer Handbook*; John Wiley: New York, 1999.

MA051228F